Hindawi Publishing Corporation
ISRN Mechanical Engineering
Volume 2013, Article ID 490750, 6 pages
http://dx.doi.org/10.1155/2013/490750

Research Article

Plastic Constitutive Model and Analysis of Flow Stress of 40Cr Quenched and Tempered Steel

Wang Xiao-qiang,[1] Zhu Wen-juan,[1] Cui Feng-kui,[1] and Li Yu-xi[2]

[1] *School of Mechatronics Engineering, Henan University of Science and Technology, Luoyang 471003, China*
[2] *School of Mechanical and Precision Instrument Engineering, Xi An University of Technology, Xi An 710048, China*

Correspondence should be addressed to Zhu Wen-juan; zhuwenjuan88521@163.com

Received 6 June 2013; Accepted 10 July 2013

Academic Editors: A. Z. Sahin, A. Szekrenyes, and X. Yang

To solve the problem of the accuracy of the numerical simulations of cold rolling, the thermomechanical responses of 40Cr under uniaxial compression loading are presented. The strain rates include quasistatic ($0.004\,s^{-1}$) at temperature of 293 K and dynamic loading regime ($632\,s^{-1}$~$5160\,s^{-1}$) at temperature regime (293 K~673 K). Significant strain rate and temperature sensitivity are measured. Based on these observations, the Johnson-Cook phenomenological constitutive model is proposed to predict the mechanical behavior of the 40Cr over wide ranges of strain rate and temperature. The solution process of the equation parameters is given. Correlations with this Johnson-Cook model are shown very close to the observed responses. Important material parameters are provided to the application of numerical analysis in project.

1. Introduction

High-speed cold rolling is an advanced cold bulk metal forming technology. During the forming process, the workpiece is interruptedly struck by high-speed rolls, and plastic deformation of the workpiece is gradually achieved [1, 2]. 40Cr quenched and tempered steel is the main structure material used in high-speed cold rolling technology because of its good strength and ductility combination. During high-speed cold rolling forming, 40Cr quenched and tempered steel is subjected to high strain rates (about $900\,s^{-1}$~$4000\,s^{-1}$) and large deformation. Numerical analysis is a critical tool for understanding the complex deformation mechanics that occur during cold rolling forming processes. Confidence in the numerical analysis of formability depends on the accuracy of the constitutive model describing the behavior of the material. Therefore, there is a good need to characterize 40Cr quenched and tempered steel's dynamic responses and constitutive model when performing numerical analysis of high-speed cold rolling.

A large number of researches have been carried out in understanding and modeling the mechanical behavior of metals under different strain rates and temperatures in both experimental and theoretical schemes. Thermomechanical responses of H13 hardened steel over a strain rate range from $10^3\,s^{-1}$ to $10^4\,s^{-1}$ and a temperature range of 293 K to 673 K was investigated by Lu and He [3]. In their study, the determination of the Johnson-Cook material parameters of H13 hardened steel was based on the experimental results. The Johnson-Cook (JC) constitutive model was shown to correlate and predict the observed responses reasonably well. The quasistatic ($10^{-3}\,s^{-1}$~$10\,s^{-1}$) and dynamic responses ($650\,s^{-1}$~$8500\,s^{-1}$) at room temperature of pure iron were investigated by Bao et al. [4]. In their study, the determination of the Johnson-Cook material parameters of pure iron was based on the experimental results. The model predictions were compared with the experimental results, and a good agreement had been observed. A systematic study of the response of Ti-6Al-4V alloy and advanced high strength steels under quasi-static and dynamic loading at different strain rates and temperatures was investigated by Khan et al. [5, 6]. In their study, the correlations and predictions using modified Khan-Huang-Liang (KHL) constitutive model were compared with those from Johnson-Cook (JC)

model and experimental observations for this strain rate and temperature-dependent material. Results showed that KHL model correlations and predictions were shown to be much closer to the observed responses than the corresponding JC model predictions and correlations. Segurado et al. [7] used a physically-based model based on self-consistent homogenization behavior to provide a texture-sensitive constitutive response of each material point, within a boundary problem solved with finite elements (FE). The resulting constitutive behavior was implemented in the implicit FE code Abaqus. The accuracy of the proposed implicit scheme and the correct treatment of rotations for prediction of texture evolution were benchmarked by experiment. The potential of the multiscale strategy was illustrated by a simulation of rolling of a face-centered cubic (FCC) plate. Voyiadjis and Abed [8] developed a coupled temperature and strain rate microstructure physically based that yield function dynamic deformations of body-centered cubic (BCC) metals. Computational aspects of the model were addressed through the finite element implementation with an implicit stress integration algorithm. Numerical implementation for a simple compression problem meshed with one element was used to validate the model. A physically based model was developed based on the mechanism of dislocation kinetics of 3003 Al-Mn alloy over a wide range of strain rates and temperatures by Guo et al. [9]. Comparing the model predictions with the experimental results, a good agreement had been observed. The flow stress of 40Cr at various deformations was studied by Li et al. [10]. In their study, an improved model suiting for hot and warm working was developed, but this study was performed over a very limited range of strain rates ($0.1\,s^{-1}$~$10\,s^{-1}$), which is not suitable for numerical simulation of high-speed cold rolling forming. Therefore, the corresponding mechanical responses of 40Cr quenched and tempered steel under different strain rates and temperatures need to be well understood.

In the current research, quasi-static loading ($0.004\,s^{-1}$) at room temperature and dynamic compression experiments over a strain rates range from $632\,s^{-1}$ to $5160\,s^{-1}$ and a temperature range of 293 K~673 K of 40Cr quenched and tempered steel were presented. Based on the experimental observations of strain rate and temperature sensitivity, Johnson-Cook (JC) constitutive model was established to describe the flow stress of 40Cr quenched and tempered steel. Determination of material constants was made. Correlations and predictions with Johnson-Cook model and experiment-observed responses were analyzed.

2. Experiment

2.1. Experimental Material and Scheme. A 40Cr quenched and tempered steel was used in the current study. All the specimens used in this study were made from the same piece of round bar stock. The specimens were machined using quenching and tempering, wire EDM, and cutting and grinding. The specimen geometry that was used in all the samples tested in this study is Φ 5 mm × 4 mm. End face of the specimen' depth of parallelism is 0.002, and the hardness is HRC 26~30.

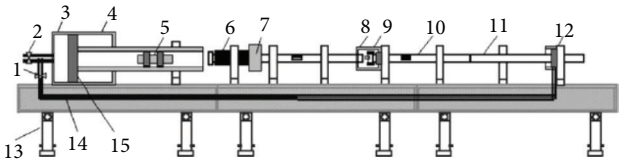

Figure 1: Schematic of compression split-Hopkinson pressure bar. (1) Outlet valve; (2) inlet valve; (3) back air chamber; (4) front air chamber; (5) strike bar; (6) incident bar; (7) reaction mass; (8) heating furnace and thermal couple; (9) specimen; (10) transmitted bar; (11) absorption; (12) driver; (13) support; (14) air pipe; and (15) plunger.

In order to analyze the dependence of flow stress on the coupled effect of strain hardening, strain rate, and temperature, five groups of dynamic compression experiments and one group of quasi-static compression were performed. Three groups of dynamic compression experiments were performed at different strain rates of $1072\,s^{-1}$, $2534\,s^{-1}$, and $5160\,s^{-1}$ at room temperature. Two groups of dynamic compression experiments were performed at the temperatures of 473 K and 673 K and at the strain rates of $1193\,s^{-1}$ and $1380\,s^{-1}$. Quasi-static compression experiments were performed at the strain rate of $0.004\,s^{-1}$ at room temperature.

2.2. Experimental Conditions. Quasi-static compression experiment was conducted using the MTS system with an axial load capacity of 250 KN. The mechanical response of 40Cr quenched and tempered steel under dynamic loading was characterized by using the compression split-hopkinson pressure Bar (SHPB) technique. The schematic of the experimental set up is shown in Figure 1. The system mainly consists of a striker bar, incident bar, and transmitted bar. The diameter and material of the striker bar was the same as that of incident and transmitted bar. All of them were remaining in a linear elastic state of stress during the test. Incident bar and transmitted bar were perfectly aligned.

Split-Hopkinson pressure bar (SHPB) technique satisfies four assumptions [11]: (1) fundamental assumption of one-dimensional stress wave propagation theory; (2) having a uniform cross section and stress distribution over the entire length; (3) ignoring friction; and (4) ignoring inertia.

2.3. Experimental Procedures

2.3.1. Quasi-Static Uniaxial Compression Experiments. Quasi-static tensile experiments were performed at room temperature. Constant velocity of the testing machine was 20 mm/min. The specimen-gripping portion is clamped by friction force between the wall of the fixture and the wall of the hardened steel block. A high elongation uniaxial strain gage, bonded on the gage section of the specimen, was used to measure strain. The strain of this experiment was achieved at 31.5%. The load obtained from the MTS load transducer was used to calculate the stress. The strain rate of this experiment which was calculated from the engineering strain and time was $0.004\,s^{-1}$. In all the experimental results discussed in

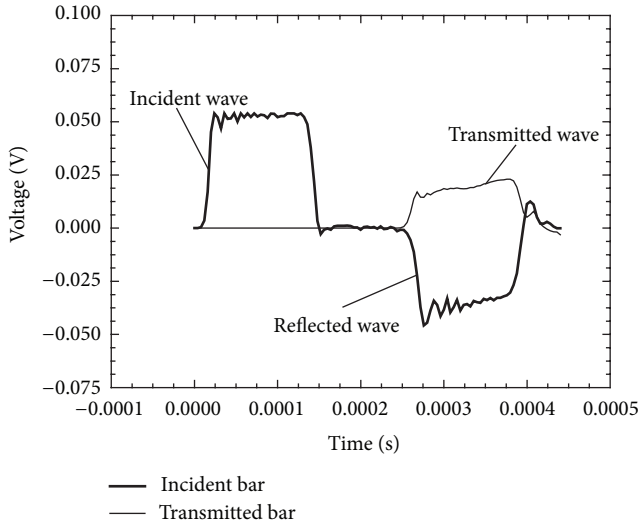

Figure 2: Pulse of 40Cr quenched and tempered steel' dynamic compression experiment.

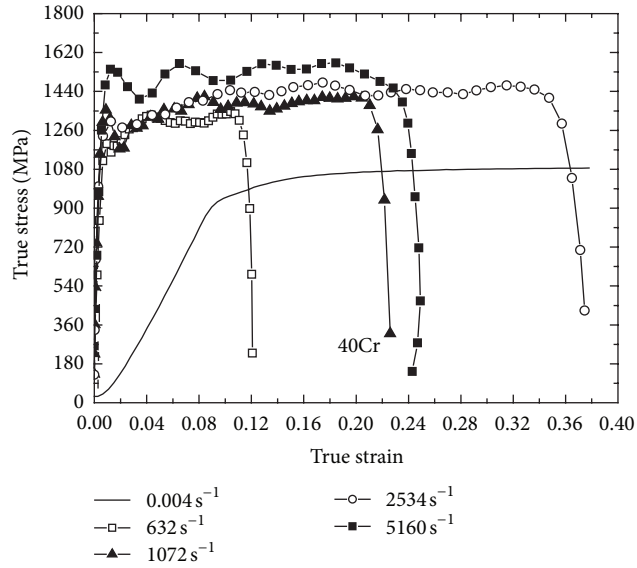

Figure 3: The measured responses of 40Cr under compression experiments at different strain rates and at 293 K.

this study, the true stress-strain responses of the material are calculated from their engineering stress-strain relationship.

2.3.2. Dynamic Compression Experiments at Different Strain Rates and Temperatures. The specimen was sandwiched between the input and output bars. The required strain rates were obtained through adjusting the gage lengths of the strike bar and the pressure of the gas gun. The dynamic compression experiment was conducted by pressuring the gas gun and releasing the solenoid valve. This results in imparting high speed motion to the projectile sitting in the gas gun. The high speed projectile impacts the incident bar generating compression waves in the incident bar and in the projectile. When the stress wave reaches the interface between the incident bar and the specimen, due to the impedance mismatch at the incident bar-specimen interface, part of the incident pulse is reflected back (reflected pulse) into the incident bar, and the rest is transmitted into the specimen. There will be further reflections and transmissions within the specimen and a compressive pulse gets transmitted into the transmitter bar (transmitted pulse) (see Figure 2). The strain gages bonded on the incident and transmitted bar measures the elastic deformation of the bars which were later converted to plastic strains on the specimen using one-dimensional wave theory.

3. Experimental Results and Discussion

3.1. Strain Rate Sensitivity. The true stress and true strain curves from the uniaxial compression experiments at strain rates of 0.004 s^{-1}, 632 s^{-1}, 1072 s^{-1}, 2534 s^{-1}, and 5160 s^{-1} and at the temperature of 293 K are shown in Figure 3. 40Cr quenched and tempered steel showed positive strain-rate sensitivity. Compared with quasi-static experiment, it was observed that the flow stress and elastic modulus of 40Cr quenched and tempered steel under dynamic condition were significantly increased and that the plastic deformation was earlier. Under high strain rates, with the increase of strain, the true stress and true strain curves are close to ideal elastic-plastic model. The reason for this phenomenon is that the plastic deformation of 40Cr quenched and tempered steel in high strain rate is of adiabatic nature. Thermal softening and hardening of the material interact with each other. The work hardening rate in 40Cr quenched and tempered steel increased with strain, and at the same time, the work hardening rate in 40Cr quenched and tempered steel decreased with increase in temperature. In addition, with the increase of strain, the effect thermal softening played on flow stress was larger than hardening.

3.2. Temperature Sensitivity. The true stress and true strain curves from the uniaxial compression experiments at temperatures of 293 K, 473 K, and 673 K and at strain rate around 1000 s^{-1} are shown in Figure 4. 40Cr quenched and tempered steel showed positive temperature sensitivity. The true stress and true strain curves all experience a sudden rise and declining procedure. This illustrates that dramatic gliding happened in the initial deformation of material. The reason for gliding is the movement of dislocation. Around each 200 K increase of temperature, the flow stress of 40Cr quenched and tempered steel is of obvious decrease. This is because temperature has a pronounced effect on the flow stress. With the temperature increase, capacity for action of the atom is more active, the movement of dislocation is easier, and hardening caused by pilling up of dislocations is weaker. So, the resistance of material deformation decreased, while thermal softening increased obviously. The higher the temperature, the more obvious thermal softening is, the more flat the curve.

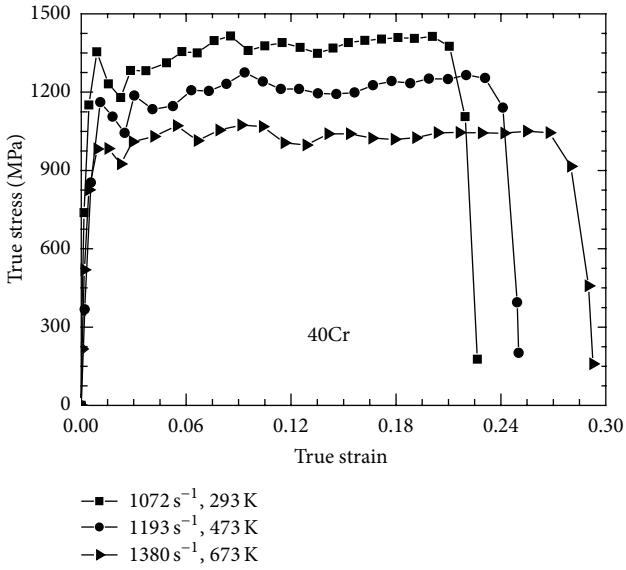

Figure 4: The measured responses of 40Cr under compression experiments at different temperatures and at strain rate around $1000\,s^{-1}$.

4. Constitutive Modeling

A constitutive relation needs to define the dependence of flow stress on the coupled effect of strain hardening, strain rate, and temperature. The flow stress is observed to be a function of plastic strain, strain rate and temperature. These dependencies are usually expressed as multiplicative terms as follows:

$$\sigma(\varepsilon, \dot{\varepsilon}, T) = \sigma_0(\varepsilon, \dot{\varepsilon}, T)\, g(\dot{\varepsilon}, T)\, h(T). \quad (1)$$

4.1. Establishment of Constitutive Modeling. Johnson-Cook model, which has the capability to mathematically describe the mechanical responses of the material when it is subject to loadings under different strain rates and temperatures, is a purely phenomenological model. This model is used frequently in engineering structures due to its advantage of fewer constants, suitability of various crystal structures, and its ability to model the observed material response as closely as with models with many more constants [12]. Based on the previous analysis, it can be seen that this model is suitable to describe the flow stress of 40Cr quenched and tempered steel.

The JC model is given by the following equation:

$$\sigma = \left[A + B\left(\varepsilon^p\right)^n\right]\left(1 + C\ln\dot{\varepsilon}^*\right)\left(1 - T^{*m}\right), \quad (2)$$

where σ is the stress and ε^p is the plastic strain. T, T_m, and T_r are current, melting, and reference temperatures, respectively. The five material constants are A, B, n, C, and m. $\dot{\varepsilon}^* = \dot{\varepsilon}^p/\varepsilon_0$ is the dimensionless plastic strain rate for $\dot{\varepsilon}_0 = 0.004\,s^{-1}$ and $T^* = (T - T_r)/(T_m - T_r)$ is the homologous temperature for $T_r = 293\,K$. The expression in the first set of brackets gives the stress as a function of strain for $\dot{\varepsilon}^* = 1.0$ and $T^* = 0$. The expressions in the second and third sets of brackets represent the effects of strain rate and temperature, respectively.

4.2. Determination of Material Constants

4.2.1. Determination of Constant n and B. Strain hardening exists in the process of 40Cr quenched and tempered steel quasi-static compression experiment. The material constants of A, B, and n should be obtained from data of quasi-static compression experiment at room temperature. At reference temperature ($T = 239\,K$) and reference strain rate ($\dot{\varepsilon} = 0.004$), (2) can be expressed as

$$\sigma = A + B\varepsilon^n. \quad (3)$$

The constitutive model of 40Cr quenched and tempered steel at quasi-static and room temperature is (3). Take the logarithm of both sides of (3):

$$\ln(\sigma - A) = \ln B + n\ln\varepsilon. \quad (4)$$

The relationship between $\ln(\sigma - A)$ and $\ln\varepsilon$ can be given by (4). $\ln B$ is the intercept and n is the slope of the fitting line in the $\ln(\sigma - A) - \ln\varepsilon$ plot. The value of A is calculated from the yield stress $\sigma_{0.085} = 905\,MPa$. The value of n and B can be obtained as 0.26 and 226 MPa from the fitting of the work hardening experiment data under quasi-static condition at room temperature.

4.2.2. Determination of Constant C. In order to obtain the material constant of C, data of dynamic compression experiments are needed. At reference temperature, there is no flow softening term as $T^* = 0$, and (2) can be expressed as

$$\sigma = \left(A + B\varepsilon^n\right)\left(1 + C\ln\dot{\varepsilon}^*\right). \quad (5)$$

Further expressed as

$$\frac{\sigma}{A + B\varepsilon^n} = 1 + C\ln\dot{\varepsilon}^*. \quad (6)$$

The relationship between $\sigma/(A + B\varepsilon^n)$ and $\ln\dot{\varepsilon}^*$ can be obtained. The material constant C can be evaluated as 0.03 by linear fitting of the experiment data. These data are the true stress at the strain rates of $632\,s^{-1}$, $1072\,s^{-1}$, and $5167\,s^{-1}$. For each true stress, the true strain is 0.1.

4.2.3. Determination of Constant m. Thermal softening constant means the dependence of flow stress on temperature. The determination of constant m needs the dynamic experiment data at elevated temperatures. At reference temperature and reference strain rate, take the logarithm of both sides of (2), it can be expressed as:

$$\ln\left[1 - \frac{\sigma}{\left(A + B\varepsilon^n\right)\left(1 + C\ln\left(\dot{\varepsilon}/\varepsilon_0\right)\right)}\right] = m\ln T^*. \quad (7)$$

It can be seen that m is the slope of the straight, and m can be obtained as 0.83 by linear fitting of the experiment data. These data are the true stress at the strain rates of $1124\,s^{-1}$, $1193\,s^{-1}$, $1236\,s^{-1}$ and $1380\,s^{-1}$ at the temperatures of 373 K, 473 K, 573 K, and 673 K. For each true stress, the true strain is 0.1.

By using the obtained constants of Johnson-Cook constitutive model, flow stress of 40Cr quenched and tempered steel can be expressed as

$$\sigma = \left(905 + 226\varepsilon^{0.21}\right)\left(1 + 0.03\ln\frac{\dot{\varepsilon}}{0.004}\right)\left[1 - \left(T^*\right)^{0.83}\right]. \tag{8}$$

4.3. Correlations with the Constitutive Model. As for the dynamic data of 40Cr quenched and tempered steel, thermal softening from the adiabatic deformation was effectively considered by converting the increment of temperature from the stress-strain curve using following equation:

$$\Delta T = \frac{\beta}{\rho C_p}\int_0^{\varepsilon^p}\sigma\left(\varepsilon^p\right)d\varepsilon^p, \tag{9}$$

where β, $\rho(7.87\,\mathrm{kg/m^3})$, $C_p[470J/(\mathrm{kg}\cdot\mathrm{k})]$ are the fraction of heat dissipation caused by the plastic deformation, mass density, and specific heat at constant pressure, respectively. The value of b is normally assumed as 0.9 for metals.

Use of the Johnson-Cook constitutive model defined in (2) allows (9) to be written as

$$\begin{aligned}\Delta T &= \frac{\beta}{\rho C_p}\int_0^{\varepsilon^p}\sigma\left(\varepsilon^p\right)d\varepsilon^p \\ &= \frac{\beta}{\rho C_p}\int_0^{\varepsilon^p}\left[A + B\left(\varepsilon^p\right)^n\right]\left[1 + C\ln\left(\dot{\varepsilon}\right)^*\right]\left[1 - \left(T^*\right)^m\right]d\varepsilon^p \\ &= \frac{\beta\varepsilon^p}{\rho C_p}\left[A + \frac{B}{n+1}\left(\varepsilon^p\right)^{n+1}\right]\left[1 + C\ln\left(\dot{\varepsilon}\right)^*\right]\left[1 - \left(T^*\right)^m\right].\end{aligned} \tag{10}$$

Substituting temperature increment (10) with parameters results in the temperature increment (10) taking the following form:

$$\begin{aligned}\Delta T = {} & \frac{0.9\varepsilon^p}{0.787\times 4.7}\left[905 + \frac{226}{0.26+1}\left(\varepsilon^p\right)^{0.26+1}\right] \\ & \times\left[1 + 0.03\ln\left(\dot{\varepsilon}\right)^*\right]\left[1 - \left(T^*\right)^{0.83}\right].\end{aligned} \tag{11}$$

The correlations of flow stress and temperature increase during a compression test at a nominal strain rate of $2534\,\mathrm{s^{-1}}$ at room temperature are shown in Figure 5. It can be observed that the correlations and prediction from the model were close to the experimental results. This provided a theoretical basis and material parameters for further numerical simulation of coupled thermo-mechanical finite element models.

The JC model correlations of the experimental data obtained at different temperatures and at strain rate around $1000\,\mathrm{s^{-1}}$ is shown in Figure 6. It can be observed that the flow stress level as well as the work hardening rate decreases continuously with the increase of temperature. Further, the predictions from the constitutive model were in good agreement with the experimental results.

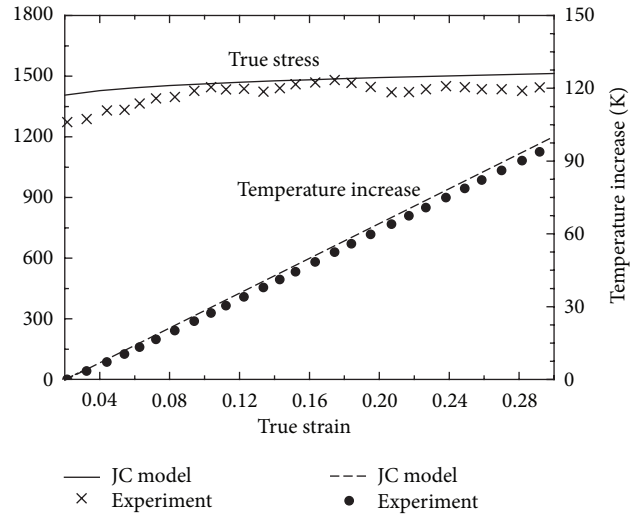

Figure 5: Flow stress and temperature increase during a compression test at a nominal strain rate of $2534\,\mathrm{s^{-1}}$ at room temperature.

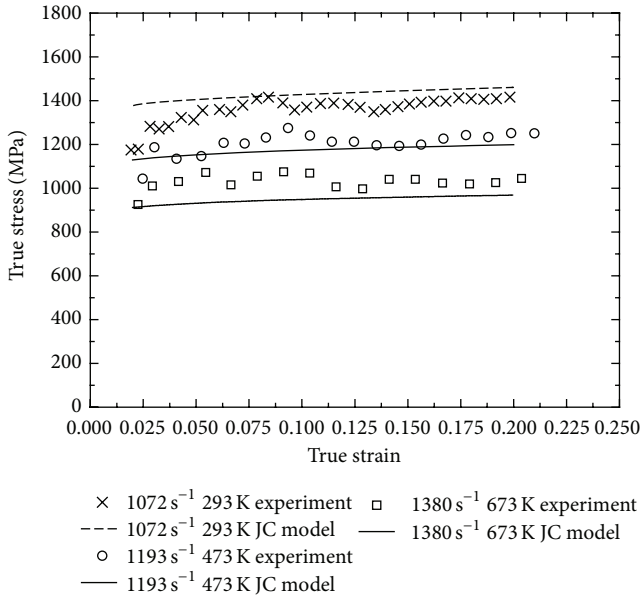

Figure 6: The JC model correlations of the experimental data obtained at different temperatures and at strain rate around $1000\,\mathrm{s^{-1}}$.

5. Conclusions

(1) Comparing dynamic experiment with quasi-static experiment, it can be observed that the flow stress under dynamic condition is much higher. 40Cr quenched and tempered steel showed positive strain-rate sensitivity.

(2) It can be observed from dynamic experiments that the flow stress 40Cr quenched and tempered steel shows positive strain-rate and temperature sensitivity. The flow stress increase with the strain rates increase, and

decrease with the increase of temperature simultaneously. Further, the flow stress showed positive thermal softening at elevated temperatures.

(3) The time of the dynamic compression experiments for 40Cr quenched and tempered steel was short, and 90% of heat dissipation was caused by the plastic deformation, which resulted in a temperature increase in specimen. The highest temperature at the strain rate of $2534\,s^{-1}$ was around 100 K. Thermal softening of material increased with the increase of strain and strain rates. The true stress and true strain curve at the strain rate of $5160\,s^{-1}$ was close to ideal elastic-plastic model.

(4) It can be observed that the correlations and prediction from the model were close to the experimental results. Johnson-Cook can preferably describe the effect of strain hardening, strain rate and temperature of 40Cr quenched and tempered steel. This provided a theoretical basis and material parameters for further numerical simulation of coupled thermo-mechanical finite element models.

Acknowledgments

The authors acknowledge the financial support of National Natural Science Foundation of China (51075124), (50975229), and the Aviation Science Fund (2009ZE54010).

References

[1] J. Quan, F. Cui, J. Yang, H. Xu, and Y. Xue, "Numerical simulation of involute spline shaft's cold-rolling forming based on ANSYS/LS-DYNA," *China Mechanical Engineering*, vol. 19, no. 4, pp. 419–427, 2008.

[2] L. Yan, Y. Mingshun, Y. Qilong, and Z. Jianming, "Study on the metal flowing of lead screw cold roll-beating forming," *Advanced Science Letters*, vol. 4, no. 6-7, pp. 1918–1922, 2011.

[3] S. Lu and N. He, "Experimental investigation of the dynamic behavior of hardened steel in high strain rate and parameter fitting of constitutive equation," *China Mechanical Engineering*, vol. 19, no. 19, pp. 2382–2385, 2008.

[4] W.-P. Bao, X.-P. Ren, and Y. Zhang, "The characteristics of flow stress and dynamic constitutive model at high strain rates for pure iron," *Journal of Plasticity Engineering*, vol. 16, no. 5, pp. 125–129, 2009.

[5] A. S. Khan, M. Baig, S.-H. Choi, H.-S. Yang, and X. Sun, "Quasi-static and dynamic responses of advanced high strength steels: experiments and modeling," *International Journal of Plasticity*, vol. 30-31, pp. 1–17, 2012.

[6] A. S. Khan, Y. S. Suh, and R. Kazmi, "Quasi-static and dynamic loading responses and constitutive modeling of titanium alloys," *International Journal of Plasticity*, vol. 20, no. 12, pp. 2233–2248, 2004.

[7] J. Segurado, R. A. Lebensohn, J. Llorca, and C. N. Tomé, "Multiscale modeling of plasticity based on embedding the viscoplastic self-consistent formulation in implicit finite elements," *International Journal of Plasticity*, vol. 28, no. 1, pp. 124–140, 2012.

[8] G. Z. Voyiadjis and F. H. Abed, "A coupled temperature and strain rate dependent yield function for dynamic deformations of bcc metals," *International Journal of Plasticity*, vol. 22, no. 8, pp. 1398–1431, 2006.

[9] W. G. Guo, X. Q. Zhang, J. Su, Y. Su, Z. Y. Zeng, and X. J. Shao, "The characteristics of plastic flow and a physically-based model for 3003 Al-Mn alloy upon a wide range of strain rates and temperatures," *European Journal of Mechanics, A/Solids*, vol. 30, no. 1, pp. 54–62, 2011.

[10] X. Li, H.-B. Zhang, X.-Y. Ruan, Z.-H. Luo, and Y. Zhang, "Analysis and modeling of flow stress of 40Cr steel," *Cailiao Gongcheng/Journal of Materials Engineering*, no. 11, pp. 41–49, 2004.

[11] M. A. Kariem, J. H. Beynon, and D. Ruan, "Misalignment effect in the split Hopkinson pressure bar technique," *International Journal of Impact Engineering*, vol. 47, pp. 60–70, 2012.

[12] G. R. Johnson and W. H. Cook, "A constitutive model and data for metals subjected to large strains, high strain rates and high temperatures," in *Proceedings of the 7th International Symposium on Ballistic*, p. 541, The Hague, The Netherlands, 1983.